[6] McClure, J. D., "On Perturbed Boundary Layer Flows," Fluid Dynamic Research Lab. Rept. 62-2, July 1962, MIT, Cambridge, Mass.

[7] Lighthill, M. J., "Reflection at a Laminar Boundary Layer of a Weak Steady Disturbance to a Supersonic Stream, Neglecting Velocity and Heat Conduction," *Quarterly Journal of Mechanics and Applied Mathematics*, Vol. 3, No. 3, March 1950, pp. 302–325.

[8] Lighthill, M. J., "On Boundary Layers and Upstream Influence II Supersonic Flows Without Separation," *Proceedings of the Royal Society*, Vol. 217, 1953, pp. 478–507.

[9] Benjamin, T. B., "Shearing Flow Over a Wavy Boundary," *Journal of Fluid Mechanics*, Vol. 6, No. 2, 1959, pp. 161–205.

[10] Lees, L. and Reshotko, E., "Stability of the Compressible Laminar Boundary Layer," *Journal of Fluid Mechanics*, Vol. 12, No. 4, 1962, pp. 555–590.

[11] Inger, G. R., "Discontinuous Supersonic Flow Past an Ablating Wavy Wall," *AIAA Journal*, Vol. 7, No. 4, April 1969, pp. 762–764.

[12] Inger, G. R., "Rotational Inviscid Supersonic Flow Past a Wavy Wall," *Bulletin of the American Physical Society*, Vol. 13, No. 11, Nov. 1968, p. 1579.

[13] Martellucci, H., Rie, H., and J. F. Somtowski, J. F., "Evaluation of Several Eddy Viscosity Models through Comparison with Measurements in Hypersonic Flows," AIAA Paper 69-688, San Francisco, Calif., 1969.

[14] Brown, W. B., "Stability of Compressible Boundary Layers," *AIAA Journal*, Vol. 5, No. 10, Oct. 1967, pp. 1753–1759.

[15] Lew, H. G. and Li, H., "The Role of the Turbulent Viscous Sublayer in the Formation of Surface Patterns," Rept. R68SD12, June 1968, General Electric Missle and Space Div., Valley Forge, Pa.

[16] Klein, E. J., "Liquid Crystals in Aerodynamic Testing," *Astronautics and Aeronautics*, Vol. 6, No. 7, July 1968, pp. 20–25.

[17] Williams, E. P. and Inger, G. R., "Investigations of Ablation Surface Cross Hatching," SAMSO TR-70-246, June 1970, McDonnell Douglas Astronautics, Huntington Beach, Calif.

MAY 1972 AIAA JOURNAL VOL. 10, NO. 5

Boundary-Layer Separation on Slender Cones at Angle of Attack

KENNETH F. STETSON*
Aerospace Research Laboratories, Wright-Patterson Air Force Base, Ohio

Experimental results of hypersonic laminar boundary-layer separation on cones at angle of attack were obtained in a $M_\infty = 14.2$ wind tunnel with a 5.6° half-angle cone model with sharp and spherically blunt tips. Based on data consisting of surface pressure measurements, Pitot pressure surveys, and surface oil flow patterns, a new model for hypersonic three-dimensional separation is proposed. This model, for both sharp and blunt cones, contains symmetrical supersonic helical vortices with an attachment line on the most leeward ray and resembles Maskell's free vortex layer type of separation. For the blunt cone the separation lines appear to orginate in the region where the lateral component of skin friction is zero. The vortices are close to the surface (at least up to $\alpha = 18°$) and there is no subsonic reverse flow associated with the vortex pattern.

Nomenclature

L = total model surface length
M_∞ = freestream Mach number
p_B = base pressure
p = cone surface pressure
p_∞ = freestream pressure
p_o = wind-tunnel reservoir pressure
p_{st} = stagnation pressure on model
p_{T_2} = Pitot pressure
r = radial distance from center of model base
Re_∞/ft = unit Reynolds number based on freestream conditions
R_B = model base radius
R_N = nose radius
T_o = wind-tunnel reservoir temperature
X = distance along the cone surface from the tip or from the zero angle-of-attack stagnation point
α = angle of attack
θ_c = cone half-angle
ϕ = cone circumferential angle, measured in a clockwise direction based on a head-on view, with the most windward ray being designated $\phi = 0$

Presented as Paper 71-129 at the AIAA 9th Aerospace Sciences Meeting, New York, January 25–27, 1971; submitted June 3, 1971; revision received December 27, 1971.

Index categories: Boundary Layers and Convective Heat Transfer—Laminar; Supersonic and Hypersonic Flow; Jets, Wakes, and Viscid-Inviscid Flow Interactions.

* Aerospace Engineer, Fluid Dynamics Facilities Research Laboratory. Associate Fellow AIAA.

Introduction

THE leeward region of a slender body at angle of attack has associated with it a complex viscous-inviscid interaction and may include a three-dimensional separated flowfield. Considerable progress has been made in calculating three-dimensional flowfields about cones at angle of attack for the case of an attached boundary layer[1–6]; however, these techniques have not proven capable of making an adequate prediction of boundary-layer separation or producing a solution downstream of separation. Limited experimental data[7–12] have only partially defined the leeward flowfield characteristics. Although these investigations had significantly increased the general understanding of flowfields about cones at angle of attack, it was not possible from these findings to establish an appropriate flowfield model for three-dimensional separation.

Maskell[13] has identified several possible models for three-dimensional separation on a body of revolution at angle of attack; however, their occurrence in given physical situations remains to be determined. The three-dimensional separation bubble has been considered by many investigators to be the most likely flowfield model for separation on a blunt cone at angle of attack. A pictorial representation of this model of separation is shown in Fig. 1. Significant features of this model are a separation line which originates from a singular point on the most leeward generator and a separated layer enclosing a "bubble". Upstream of the separation bubble the leeward flowfield is nose-dominated, with large favorable pressure gradients, and the boundary layer is attached. The bubble contains subsonic flow traveling upstream

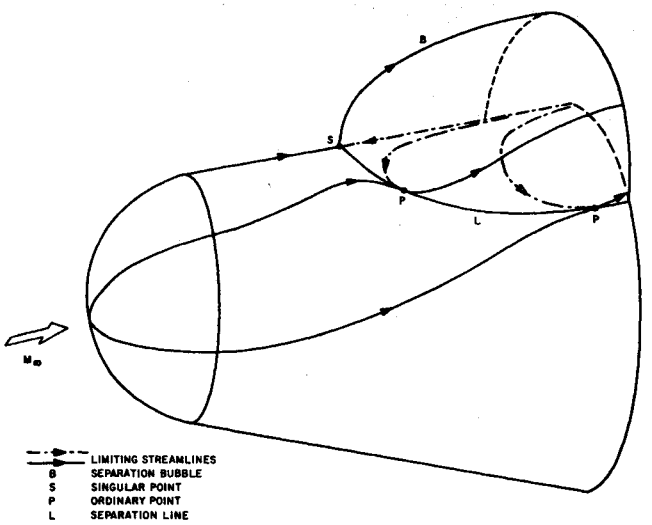

Fig. 1 Separation bubble flowfield model for three-dimensional separation.

from the base. For this mode of separation subsonic communication exists between the bubble and the base region. One objective of this present investigation was to experimentally determine if a separation bubble formed on a blunt cone at angle of attack in a hypersonic flow.

A significant feature to be considered in describing three-dimensional separated flowfields is the influence of the base region. It is important to determine if separation on the leeward side of a cone is initiated by a downstream condition established by the base region, yet this point has received little attention. The aspect of communication between the separated flowfield in the leeward region and the separated flowfield associated with the base was briefly explored in Ref. 14. Figure 2 (from Ref. 14) shows schematically the separated flowfields associated with a cone at angle of attack. Region I represents the separated region which is associated with the leeward side of the cone and Region II represents the separated region associated with the base of the cone. It might logically be concluded, based upon knowledge obtained mainly from two-dimensional studies, that these two separated regions must be tied together and that subsonic communication between the two regions would result in a nearly equal pressure throughout. This is certainly the case at very high angles of attack (e.g., $\alpha \to 90°$) where both flowfields merge into one base flow-type region. It was found[14] that two types of separated flow situations may be associated with a cone at angle of attack. In one case there is no significant communication between the two separated regions and the pressures on the leeward surface of the cone are always larger than base pressure.

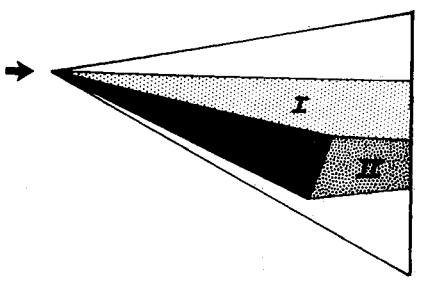

Fig. 2 Schematic representation of separated flowfields associated with a cone at angle of attack.

The leeward separated flowfield for this case is analogous to that of an infinitely long cone. At angles of attack greater than that which was required to equalize base and leeward pressures a new flow feature was observed, producing the second separated flow case, the "base interference" case. This case involved an interaction of the two separated regions and the appearance of a secondary separation on the rear portion of the cone leeward surface.

The objective of this present investigation was to obtain experimental data which would clarify the main features of separated flow on cones at angle of attack and to define the basic features of an appropriate flowfield model. Additional details of this investigation can be found in Refs. 15 and 16.

Model, Instrumentation and Test Facility

Model

The model used was a sting-mounted, 5.6° half-angle cone with two nose tip configurations, a sharp tip and a blunt tip with a nose radius equal to 30% of the base radius. The sharp tip had a tip diameter slightly over 0.001 in. The model base diameter was three inches and the sting diameter was one inch. The cone circumferential angle (ϕ) was measured in a clockwise direction based on a head-on view, with the most windward ray being designated $\phi = 0$. The cone surface was instrumented with pressure orifices along a cone ray, with additional pressure orifices for checking aerodynamic alignment and for measuring base pressures. Complete cone surface pressure distributions were obtained by rotating the model about its axis between runs.

Instrumentation

Surface pressures were measured with variable reluctance differential pressure transducers that responded linearly with pressure. Repeated calibration of these transducers have indicated that they are accurate to about $\pm 2\%$ of measured values. These pressure transducers are discussed in detail in Ref. 17.

A simple Pitot probe was constructed for Pitot pressures surveys. This probe was made with 0.072 o.d. pressure tubing (0.054 i.d.) with a 1-in. knife edge for support and stream-lining. The tube extended two inches beyond the knife edge and had a 10° internal bevel at the open end. The probe was mounted on the wind axis system (i.e., the axis of the probe was parallel to the direction of the freestream velocity vector and the probe traverses were made in a plane normal to the freestream velocity vector). The Pitot probe was made relatively large to reduce the response time and two pressure transducers were utilized (one that would accurately measure pressures of the order of 1 mm of mercury and a second transducer to measure the higher pressures). The Pitot probe was first brought in to the cone surface and left there for several seconds until a steady pressure was observed, then a slow outward traverse was made, requiring about three minutes to complete.

The oil formula used for the oil flow experiments was as

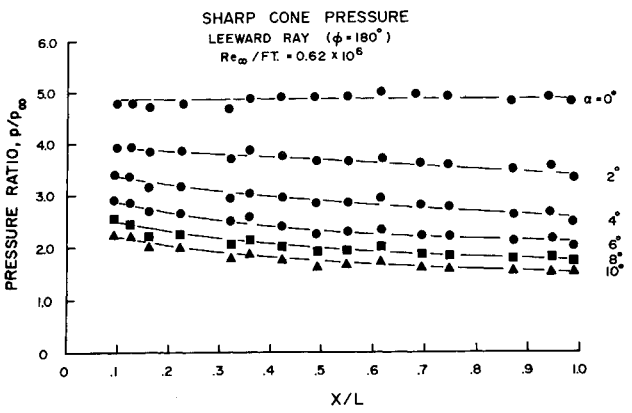

Fig. 3 Sharp cone pressure distributions along most leeward ray.

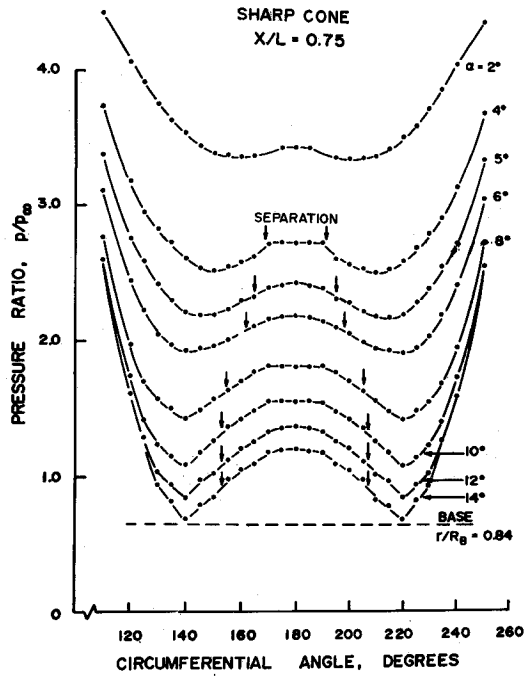

Fig. 4 Sharp cone circumferential pressure distributions at $X/L = 0.75$.

follows: Silicone oil, 7 cc—10 centistokes, 3 cc—100 centistokes; Titanium dioxide, 3 cc; Oleic acid, 2 drops.

Several oil application patterns were tried (dots, circumferential strips, and longitudinal strips) and generally the best results were obtained by applying the oil with a brush in longitudinal strips in the windward region in conjunction with several circumferential strips in the leeward region. The tests were visually observed through the tunnel window to determine when to terminate the run. Run times were typically about 2 min.

Test Facility

The experiments were conducted in the ARL 20-in. wind tunnel at a Mach number of 14.2 and a freestream Reynolds number/ft of 0.62×10^6. Average test conditions were as follows: $p_o = 1600$ psia; $T_o = 2050°$R; $p_\infty = 0.0032$ psia; $p_{st} = 0.85$ psia. The ratio of wall-to-total temperature was approximately 0.29 for these experiments. A more complete description of this test facility can be found in Ref. 18.

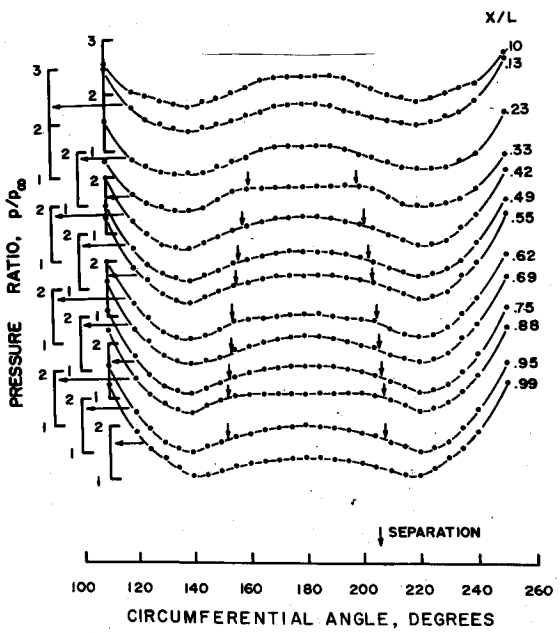

Fig. 5 Sharp cone circumferential pressure distributions at $\alpha = 10°$.

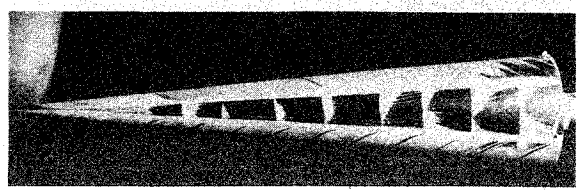

Fig. 6 Oil flow photograph, leeward view, sharp tip, $\alpha = 10°$.

Results

Cone surface pressure and surface oil flow patterns were obtained at angles of attack up to 18° and Pitot pressure surveys were made at several angles, with most of the Pitot pressure data being obtained at 10° angle of attack. Samples of cone surface pressure distributions along rays and circumferentially are shown and representative samples of oil flow results and Pitot pressure surveys are included.

As will be discussed in more detail later, the pressure data may be intuitively interpreted as a separated flow condition, but these data, per se, do not verify that the flow is actually separated nor do they permit the location of the separation lines. Additional information is required for such separation determinations. The surface oil flow technique was found to be a simple and easy method of obtaining this important three-dimensional separation information. The surface oil flow technique is a well established method of flow visualization in wind tunnels. Since the skin-friction force causes the oil to flow, the patterns produced indicate skin-friction lines or surface streamlines. The validity of this technique has been analytically evaluated by Squire[19] and he concluded that: 1) the oil follows the boundary-layer surface streamline except near separation where it tends to form an envelope upstream of the true separation envelope; and 2) the effect of the oil flow on the motion of the boundary layer is very small. Experience has indeed indicated that the presence of the oil on the model surface has little effect on the boundary-layer flow and that the technique provides reliable information regarding surface streamline direction, boundary-layer separation and boundary-layer transition.[20] The sharp cone and the blunt cone results are presented separately.

Sharp Cone

Figure 3 shows pressure distributions along the most leeward ray ($\phi = 180°$) for several angles of attack. At zero angle of attack the cone surface pressure was constant, whereas at angle of attack a pressure gradient developed in the leeward region. Figure 4 presents an example of circumferential surface pressure distributions in the leeward region of the cone for angles of attack up to 14°. The general features of these data are similar to the data obtained by Tracy,[7] Rainbird,[8-9] and Feldhuhn, Winkelmann and Pasiuk.[12] That is, there exists symmetrical minimum pressure locations off the leeward plane of symmetry, followed by an adverse pressure gradient in the cross-flow plane. At 14° angle of attack, which is $2\frac{1}{2}$ times the cone half angle, the cone surface pressures are still greater than base pressure. This situation infers there was no subsonic communication between the cone surface and the base region and raises the question of

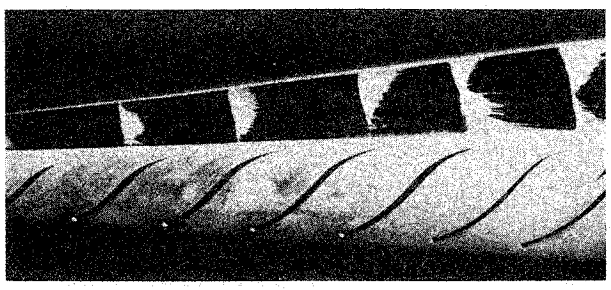

Fig. 7 Oil flow photograph, leeward and side region, sharp tip, $\alpha = 10°$.

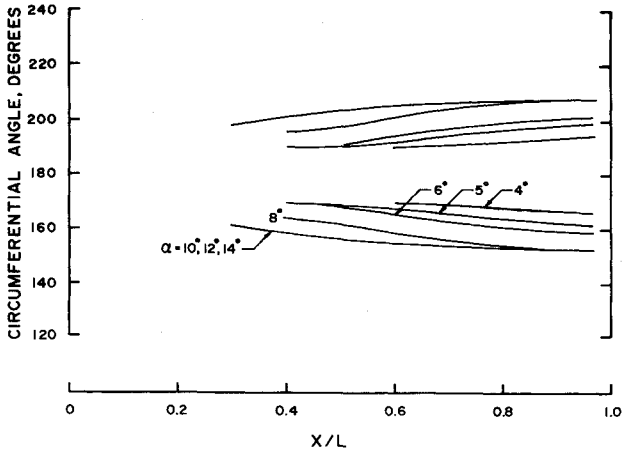

Fig. 8 Sharp cone separation angles.

whether such a flow situation would exist if the leeward separated flowfield contained subsonic reverse flow. These data are then analogous to that which would be obtained on an infinitely long cone. Additional increases in angle of attack would produce further reductions in cone surface pressures and subsequent interaction with the base flowfield.[14] The leeward base pressures were essentially constant in the angle of attack range from 0 to 14°.[21] The locations of the separation line were obtained from the oil flow photographs and are shown in Fig. 4. Incipient separation occurred at approximately 4° angle of attack, or about 70% of the cone half-angle. As the angle of attack was increased the circumferential angle at which separation occurred changed from 11 to 27° off the plane of symmetry. It does not appear possible to identify the separation lines with a unique feature of these pressure curves.

Figure 5 is an example of the circumferential pressure distribution at various positions along the cone. These data show a similarity of features throughout, which would be expected for a sharp cone. An interesting point is the curvature of the separation lines.

Figures 6 and 7 are samples of the oil flow data obtained for the sharp cone. The pattern of converging surface streamlines toward both sides of the separation line and diverging surface streamlines from the reattachment line on the leeward plane of symmetry was observed. Four degrees angle of attack appeared to be close to the incipient separation condition, with the rear portion of the cone exhibiting a fairly well developed separation line, whereas the forward half of the cone showed only an accumulation of oil in the leeward region with no definitive line. Figure 7 is a view of the leeward and side regions, looking about 45° off the leeward plane of symmetry. The distinctive cross-flow pattern on the side of the cone resulted from oil from the windward side of the cone flowing past the pressure orifices. Figure 8 contains separation angle data obtained from the oil flow

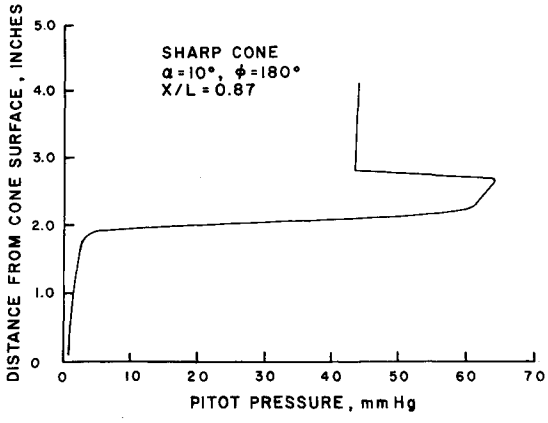

Fig. 9 Sharp cone Pitot pressure profile.

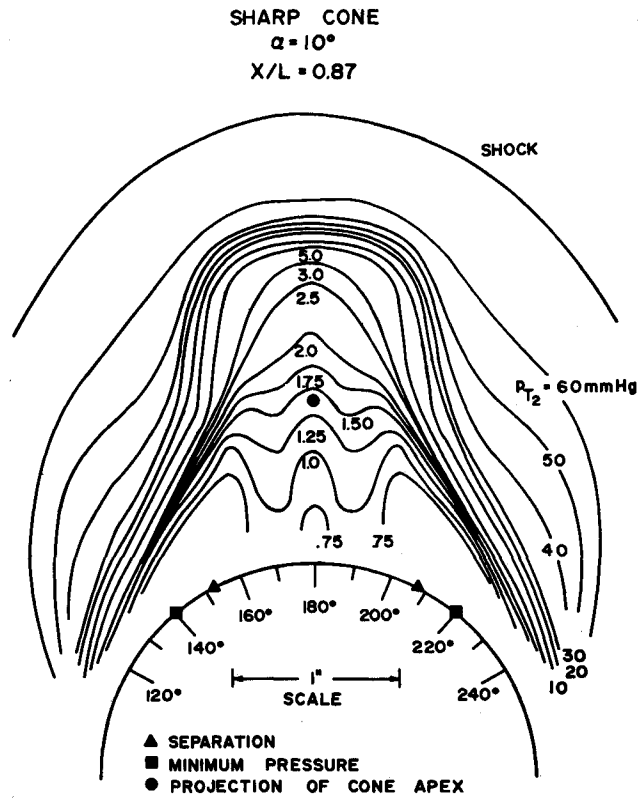

Fig. 10 Pitot pressure contours, sharp cone, $\alpha = 10°$, $X/L = 0.87$.

photographs. The separation lines exhibited curvature for all of these tests.

Pitot pressure surveys were made of the leeward region to obtain information about the flowfield. For example, supporting data were desired to confirm the previous suspicion that the vortices contained essentially supersonic flow and to obtain general information about the size of the vortices and the existence of imbedded shocks.

It was not possible in these experiments to assess the loss of Pitot pressure due to the probe angle of attack; however, such effects are believed to be small over most of the region probed, and the results are believed to be adequate for the general information desired. It was not possible to probe an attached boundary layer with this Pitot probe due to the large size of probe compared to the boundary-layer thickness.

Figure 9 is a sample of the Pitot pressure profiles obtained, going from the body surface out through the bow shock and terminating in the freestream. Schlieren instrumentation did not have sufficient sensitivity to observe the leeward portion of the bow shock. However, the shock location was obtained from the Pitot probe traverses and found to be curved in the tip region.

Figure 10 shows lines of constant Pitot pressure, obtained by making a number of Pitot probe traverses. Significant points are the large region of relatively low Pitot pressure, the symmetrical valleys of higher pressure within the aerodynamic shadow which are presumably associated with the downward flow of the twin vortices, and the absence of imbedded shocks.

In order to make approximate Mach number calculations of the leeward flowfield, with particular interest in the region where the vortices would be expected, a constant static pressure equal to the surface pressure was assumed. Using the data of Fig. 10 produced the Mach number contour lines shown in Fig. 11. Supersonic flow is indicated throughout the region. Even with an allowance for a reasonable error in static pressure this general conclusion of supersonic flow is not altered, thus further substantiating the concept of a supersonic vortex. The existence of supersonic vortices could be the reason why there was no subsonic communication between the cone attached vortices and the base region.

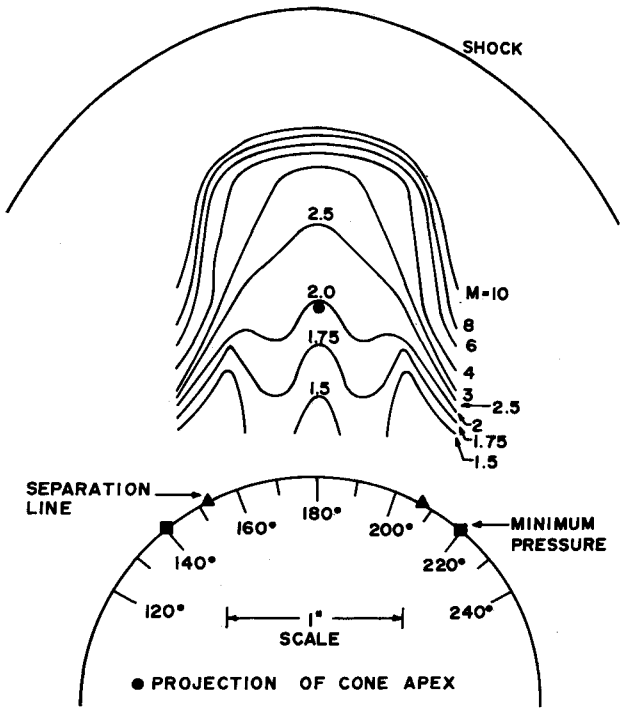

Fig. 11 Approximate Mach number contours, sharp cone, $\alpha = 10°$.

Blunt Cone

Figure 12 presents pressure distributions along several rays when the spherically blunt cone was at 10° angle of attack. Significant features are the large favorable pressure gradients in the neighborhood of the nose tip and the development of large adverse pressure gradients in the windward region from about 6–18 nose radii downstream. It will be shown later that separation on the leeward side of the cone for this condition developed in the region between about 10 and 23 nose radii downstream.

Figures 13 and 14 are examples of the circumferential pressure distributions obtained with a 30% nose bluntness. At small X/R_N's the boundary layer is attached and the minimum circumferential pressure occurs on the most leeward ray. At larger

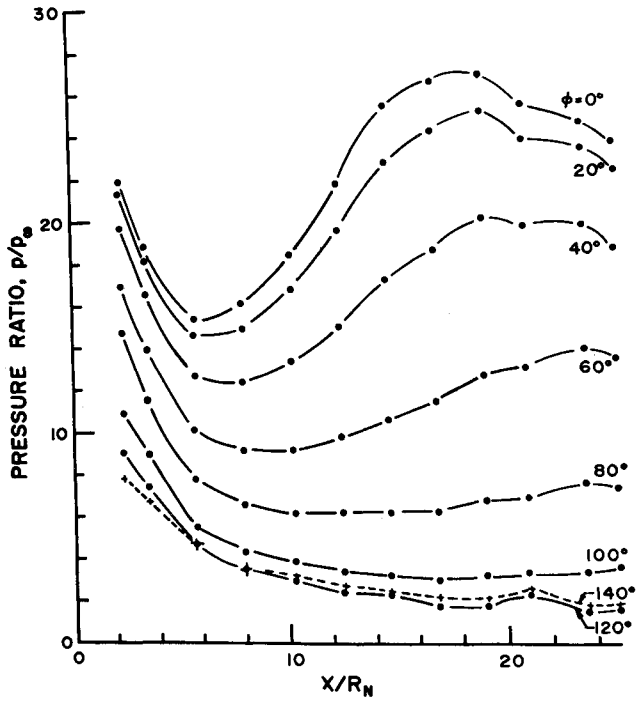

Fig. 12 Longitudinal pressure distributions, 30% bluntness, $\alpha = 10°$.

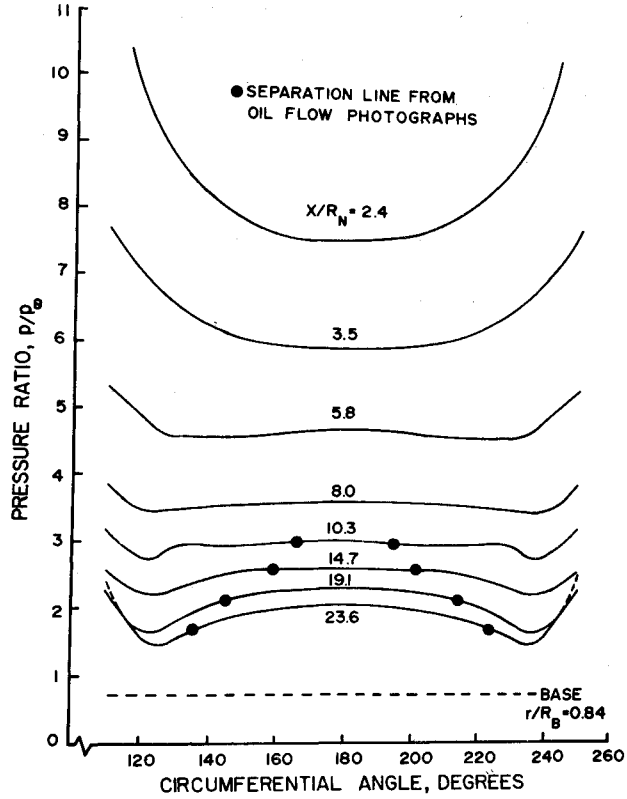

Fig. 13 Circumferential pressure distributions, 30% bluntness, $\alpha = 10°$.

X/R_N's two symmetrical minimum pressure locations occur off the leeward plane of symmetry. The points shown on the curves are separation line data obtained from the oil flow photographs. At 6° angle of attack separation occurs on the rear portion of the cone and the origin of separation occurs closer to the nose tip with increasing angle of attack. The initial portion of the separation line exhibits considerable curvature, developing in width (in

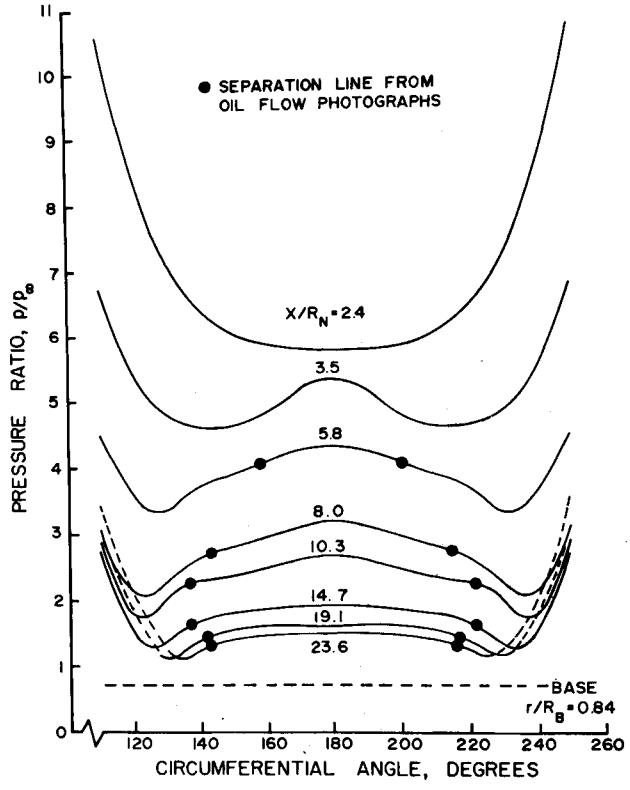

Fig. 14 Circumferential pressure distributions, 30% bluntness, $\alpha = 18°$.

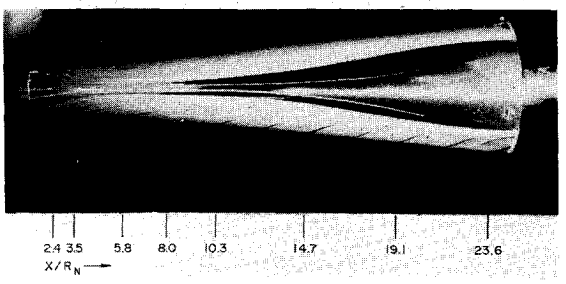

Fig. 15 Oil flow photograph, leeward view, 30% bluntness, $\alpha = 10°$.

terms of circumferential angle) to a value larger than that observed on the sharp cone, followed by a gradual reduction, apparently approaching the sharp cone value. The cone surface pressures were always larger than base pressure, even at the maximum angle of attack of 18° which was 3.2 times the cone half-angle.

Figures 15 and 16 are samples of the oil flow results with 30% nose bluntness. From observations of the tests through the tunnel window, it was seen that oil from the windward region flowed around the cone and turned toward the rear of the cone as it approached the separation lines. At the separation line the oil accumulated and proceeded to travel down the separation line to the rear of the cone. The origin of the separation lines was an interesting area to observe. There was no evidence of reverse flow and a singular point. In terms of skin friction, the leeward flow was seen initially to have a lateral component in the direction toward the leeward plane of symmetry. This lateral component of skin friction then reversed its sign as the flow traveled downstream. Two symmetrical separation lines developed downstream of the region where the lateral component of skin friction passed through zero. The longitudinal component of skin friction was always finite. This fact could be verified by observing the oil flowing from the attached region behind the nose, through the region of zero lateral skin friction, and into the vortex region. The analysis of Wang[22-23] is the only one known to this author to be compatible with this observed phenomena.

A number of Pitot pressure traverses were made in the leeward region of the 30% blunt cone at 10° angle of attack in order to construct Pitot pressure contour maps at several locations on the cone. Figure 17 shows such a map for the location of $X/R_N = 23.6$, which is in the region of maximum angular width. Significant differences between these data and the previously discussed case for the sharp cone are found in the leeward plane of symmetry and in the size and shape of the low Pitot pressure region.

Conclusions

Sharp Cone

1) Incipient separation occurred at approximately 4° angle of attack ($\alpha/\theta_c \simeq 0.7$). 2) At angle of attack the leeward region exhibited a curved bow shock wave, curved separation lines, and a longitudinal pressure gradient. 3) Pitot pressure surveys indicated a large region of low Pitot pressure in the leeward region, a supersonic flow in the region in which the presumed vortices are located, and gave no indication of imbedded shock-

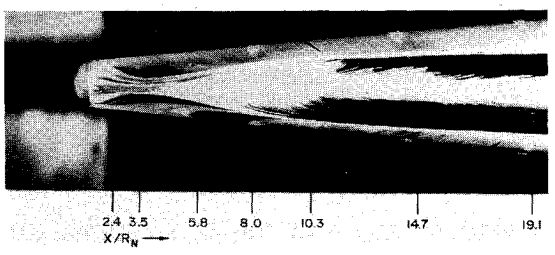

Fig. 16 Oil flow photograph, leeward view, 30% bluntness, $\alpha = 18°$.

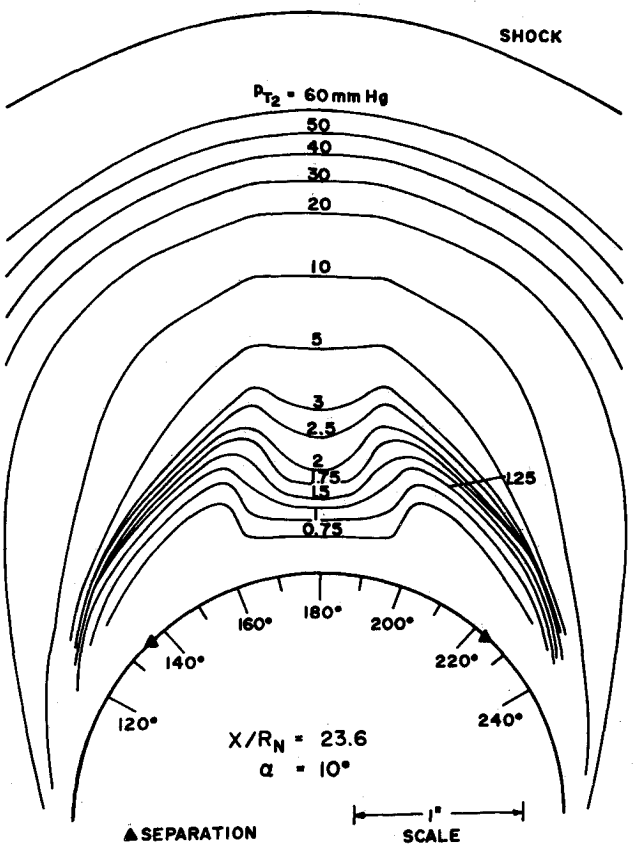

Fig. 17 Blunt cone Pitot pressure contours, $X/R_N = 23.6$, $\alpha = 10°$.

waves. 4) At $X/L = 0.75$ the angle of the separation line varied from 11° off the leeward plane of symmetry at 4° angle of attack to 27° at 14° angle of attack. 5) At 14° angle of attack, which is $2\frac{1}{2}$ times the cone half-angle, the cone surface pressures were still greater than base pressure, inferring there was no significant subsonic communication between the cone surface and the base region.

Blunt Cone

1) At small X/R_N's the cone leeward region experienced a large favorable pressure gradient with an attached boundary layer. The minimum circumferential pressure occurred on the leeward plane of symmetry and there was a lateral component of skin friction in the direction toward the plane of symmetry. At larger X/R_N's two symmetrical minimum pressure locations occurred off the leeward plane of symmetry. The lateral component of skin friction was now in a direction away from the plane of symmetry. Two symmetrical separation lines developed downstream of the region where the lateral component of skin friction passed through zero. The longitudinal component of skin friction was always finite. The origin of separation occurred closer to the nose tip with increasing angle of attack.

2) Pitot pressure surveys indicated a supersonic flow in the region of the presumed vortices and differed from the sharp cone results in the size and shape of the low Pitot pressure region and by higher pressures in the plane of symmetry.

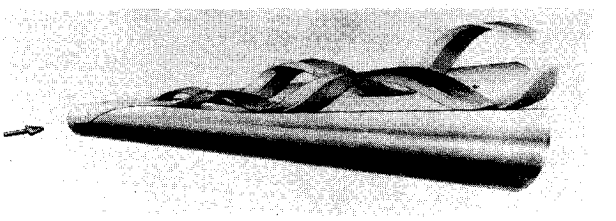

Fig. 18 Conceptual drawing of new model of boundary-layer separation on a blunt cone at angle of attack.

Based on these results a new model for hypersonic three-dimensional separation on a cone at angle of attack is proposed. This model contains symmetrical supersonic helical vortices with an attachment line on the most leeward ray and resembles Maskell's free vortex layer type of separation. The vortices are close to the surface (at least up to $\alpha = 18°$) and there is no subsonic reverse flow associated with the vortex pattern. Figure 18 is a conceptual drawing of this model of separation on a slender blunt cone at angle of attack, using "stream ribbons" to illustrate the vortex flow.

References

[1] Babenko, K. I., Voskresenski, G. P., Lyubimov, A. N. and Rusanov, V. V., "Three Dimensional Flow of an Ideal Gas Past Ideal Smooth Bodies," TT F-380, NASA.

[2] Der, J. Jr., "A Study of General Three-Dimensional Boundary Layer Problems by an Exact Numerical Method," *AIAA Journal*, Vol. 9, No. 7, July 1971, pp. 1294–1302.

[3] Moretti, G., "Inviscid Flowfield About a Pointed Cone at an Angle of Attack," *AIAA Journal*, Vol. 5, No. 4, April 1967, pp. 789–791.

[4] Gonidou, R., "Supersonic Flows Around Cones at Incidence," TT F-11, 473, Jan. 1968, NASA.

[5] Fannelop, T. K., "A Method of Solving the Three-Dimensional Laminar Boundary Layer Equations with Application to a Lifting Re-entry Body," *AIAA Journal*, Vol. 6, No. 6, June 1968, pp. 1075–1084.

[6] Boericke, R. R., "Laminar Boundary Layer on a Cone at Incidence in Supersonic Flow," *AIAA Journal*, Vol. 9, No. 3, March 1971, pp. 462–468.

[7] Tracy, R. R., "Hypersonic Flow Over a Yawed Circular Cone," GALCIT Memo No. 69, Aug. 1963, California Inst. of Technology, Pasadena, Calif.

[8] Rainbird, W. J., "Turbulent Boundary-Layer Growth and Separation on a Yawed Cone," *AIAA Journal*, Vol. 6, No. 12, Dec. 1968, pp. 2410–2416.

[9] Rainbird, W. J., "The External Flow Field about Yawed Circular Cones," *AGARD Conference Proceedings No. 30*, May 1968.

[10] Cleary, J. W., "Effects of Angle of Attack and Nose Bluntness on the Hypersonic Flow Over Cones," AIAA Paper 66-414, Los Angeles, Calif., 1966.

[11] George, O. L., Jr., "An Experimental Investigation of the Flow Field Around an Inclined Sharp Cone in Hypersonic Flow," SS-RR-69-577, Sept. 1969, Sandia Labs., Albuquerque, N. Mex.

[12] Feldhuhn, R. H., Winkelmann, A. E., and Pasiuk, L., "An Experimental Investigation of the Flow Field Around a Yawed Cone," *AIAA Journal*, Vol. 9, No. 6, June 1971, pp. 1074–1081.

[13] Maskell, E. C., "Flow Separation in Three Dimensions," Rept. 2565, Nov. 1955, Royal Aircraft Establishment, Bedford, England.

[14] Stetson, K. F. and Friberg, E. G., "Communication Between Base and Leeward Region of a Cone at Angle of Attack in a Hypersonic Flow," ARL 69-0115, July 1969, Aerospace Research Labs., Wright-Patterson Air Force Base, Ohio.

[15] Stetson, K. F. Ojdana, E. S., "Hypersonic Laminar Boundary-Layer Separation on a Slender Cone at Angle of Attack," AIAA Paper 71-129, New York, 1971.

[16] Stetson, K. F., "Experimental Results of Laminar Boundary-Layer Separation on a Slender Cone at Angle of Attack at $M_\infty = 14.2$," ARL 71-0127, Aug. 1971, Aerospace Research Labs., Wright-Patterson Air Force Base, Ohio.

[17] Murray, D. H. and Ojdana, E. S., "Low Pressure Data Acquisition Techniques in a Hypersonic Wind Tunnel," *Proceedings of the 15th ISA Aerospace Instrumentation Symposium*, May 1969, Instrument Society of America, Pittsburgh, Pa.

[18] Gregorek, G. M. and Lee, J. D., "Design Performance and Operational Characteristics of the ARL Twenty-Inch Hypersonic Wind Tunnel," ARL 62-392, Aug. 1962, Aerospace Research Labs., Wright-Patterson Air Force Base, Ohio.

[19] Squire, L. C., "The Motion of a Thin Oil Sheet Under the Boundary Layer of a Body," AGARDograph 70, April 1962, pp. 7–28.

[20] Maltby, R. L., "Flow Visualization in Wind Tunnels Using Indicators," AGARDograph 70, April 1962, Pt. I, pp. 1–74.

[21] Stetson, K. F. and Ojdana, E. S., "Base Pressures on a Sting-Mounted Cone Model at Angle of Attack at $M_\infty = 14.2$," ARL 71-0130, Aug. 1971, Aerospace Research Labs., Wright-Patterson Air Force Base, Ohio.

[22] Wang, K. C., "Three-Dimensional Laminar Boundary Layer Over Body of Revolution at Incidence," Part III, "Solutions Near the Plane of Symmetry," RIAS TR 69-14, Sept. 1969, Martin Marietta Corp., Baltimore, Md.

[23] Wang K. C., "Separation Patterns of Boundary Layer Over an Inclined Body of Revolution," AIAA Paper 71-130, New York, 1971.